

Polymerization of Nonlamellar Lipid Assemblies<sup>†</sup>Youn-Sik Lee,<sup>‡,⊥</sup> Jian-Zhong Yang,<sup>‡</sup> Thomas M. Sisson,<sup>‡</sup> David A. Frankel,<sup>‡</sup> James T. Gleeson,<sup>§,||</sup> Emre Aksay,<sup>§</sup> Sarah L. Keller,<sup>§,∞</sup> Sol M. Gruner,<sup>§</sup> and David F. O'Brien<sup>\*‡</sup>*Contribution from Carl S. Marvel Laboratories, Department of Chemistry, University of Arizona, Tucson, Arizona 85721, and Joseph Henry Laboratories, Department of Physics, Princeton University, Princeton, New Jersey 08544**Received November 28, 1994. Revised Manuscript Received January 27, 1995<sup>⊗</sup>*

**Abstract:** The formation of nonlamellar lipid structures in model lipid membranes has been extensively studied in recent years. These hydrated lipid phases include the inverted hexagonal phase and various bicontinuous cubic phases, which occur at selected lipid concentrations, temperatures, and pressures. Cubic phases that are bicontinuous with respect to the polar and nonpolar regions are especially interesting as organic analogs of zeolites. The recently developed methods used to polymerize and stabilize lamellar assemblies offer certain strategies that are applicable to nonlamellar phases. Here we report the successful stabilization of a nonlamellar phase via the polymerization of reactive amphiphiles. A 3:1 molar mixture of polymerizable mono-dienoyl-substituted phosphoethanolamine and bis-dienoyl-substituted phosphocholine were hydrated to yield bilayers. X-ray diffraction of the unpolymerized mixture at 60 °C showed the formation of an inverted hexagonal phase which on prolonged incubation changed to a bicontinuous cubic phase of  $Pn\bar{3}m$  symmetry. Polymerization of the hexagonal phase produced a stabilized hexagonal structure over the range of 20 to 60 °C. The same lipids at lower concentration were characterized by <sup>31</sup>P-NMR and transmission electron microscopy (TEM) before and after polymerization. The NMR shows the formation of a sample with isotropic symmetry as expected for a cubic phase. The polymerized sample retained a nonlamellar structure after cooling and extended storage at room temperature or near 0 °C. The TEMs show a polydomain square lattice with 6 ± 1 nm diameter aqueous channels. This stabilized nonlamellar phase is the first representative of a new family of materials with interpenetrating water channels with high surface area and potentially bicompatible lipid–water interfaces.

## Introduction

It is well-known that the hydration of purified biological lipids or their synthetic analogs yields the lamellar,  $L_\alpha$ , phase. The formation of nonlamellar lipid structures in model lipids has been extensively studied in recent years, because of the interest in the possible role of nonlamellar lipid phases in biological processes.<sup>1–3</sup> These hydrated lipid phases include the inverted hexagonal phase ( $H_{II}$ ) and various bicontinuous cubic phases ( $Q_{II}$ ) which occur at selected lipid concentrations, temperatures, and pressures. Whatever may be the biological significance of these lipid phases, there is considerable scientific and technical interest in these materials. Their potential utility depends at least in part on the prospects for stabilization of these intriguing structures in order to enlarge their useful temperature and concentration ranges. Cubic phases which are bicontinuous with respect to the polar (aqueous) and nonpolar (lipid) regions are especially appealing in this regard, because they appear to be organic analogs of zeolites. Schematic representations of

bicontinuous cubic phases belonging to two of the possible space groups are shown in Figure 1: on the left,  $Im\bar{3}m$ ; and on the right,  $Pn\bar{3}m$ .<sup>3</sup> The graphics illustrate the periodic minimum surface of the lipids (as the bilayer mid-surface) with long range order as well as the two interpenetrating aqueous channels.

The recently developed methods used to polymerize and stabilize lamellar assemblies, i.e. bilayer vesicles, offer certain strategies that should be applicable to nonlamellar assemblies. Reports of polymerizable lipids and their polymerization in lamellar phases, i.e. bilayer vesicles, started to appear in the early 1980s.<sup>4–7</sup> Since then a wide variety of polymerizable groups have been successfully employed to stabilize lamellar phases. These studies and the various strategies for polymerization of lamellar phases have been reviewed.<sup>8–11</sup> A particularly useful approach relies on the design of suitable polymerizable amphiphiles, which upon hydration form assemblies that can then be polymerized in place. Certain polymerizable lipids, e.g. diacetylenic lipids, polymerize efficiently only in the solid-analogous ( $L_\beta$ ) phase, because of the topotactic nature of the

<sup>†</sup> A preliminary description of this research was reported in: *Polym. Prepr., Am. Chem. Soc. Div. Polym. Chem.* 1994, 35, 456–457.

<sup>‡</sup> University of Arizona.

<sup>§</sup> Princeton University.

<sup>⊥</sup> Present address: Department of Chemical Technology, Chonbuk National University, Chonbuk, South Korea.

<sup>||</sup> Present address: Physics and Astronomy Departments, University of Calgary, Calgary, Canada.

<sup>∞</sup> Present address: Materials Department, University of California, Santa Barbara, CA.

<sup>⊗</sup> Abstract published in *Advance ACS Abstracts*, May 1, 1995.

(1) Lindblom, G.; Rilfors, L. *Biochim. Biophys. Acta* 1989, 988, 221–256.

(2) Seddon, J. M. *Biochim. Biophys. Acta* 1990, 1031, 1–69.

(3) Tate, M. W.; Eikenberry, E. F.; Turner, D. C.; Shyamsunder, E.; Gruner, S. M. *Chem. Phys. Lipids* 1991, 57, 147–164.

(4) Regen, S. L.; Czech, B.; Singh, A. *J. Am. Chem. Soc.* 1980, 102, 6638–6640.

(5) Johnston, D. S.; Sanghera, S.; Pons, M.; Chapman, D. *Biochim. Biophys. Acta* 1980, 602, 57–69.

(6) Hub, H.; Hupfer, B.; Koch, H.; Ringsdorf, H. *Angew. Chem., Int. Ed. Engl.* 1980, 19, 938–940.

(7) O'Brien, D. F.; Whitesides, T. H.; Klingbiel, R. T. *J. Polym. Sci.: Polym. Lett. Ed.* 1981, 19, 95–101.

(8) Ringsdorf, H.; Schlarb, B.; Venzmer, J. *Angew. Chem., Int. Ed. Engl.* 1988, 27, 113–158.

(9) O'Brien, D. F.; Ramaswami, V. *Encycl. Polym. Sci. Eng.* 1989, 17, 108–135.

(10) Singh, A.; Schnur, J. M. In *Phospholipids Handbook*; Cevc, G., Ed.; Marcel Dekker: New York, 1993; p 233.

(11) O'Brien, D. F. *Trends Polym. Sci.* 1994, 2, 183–188.

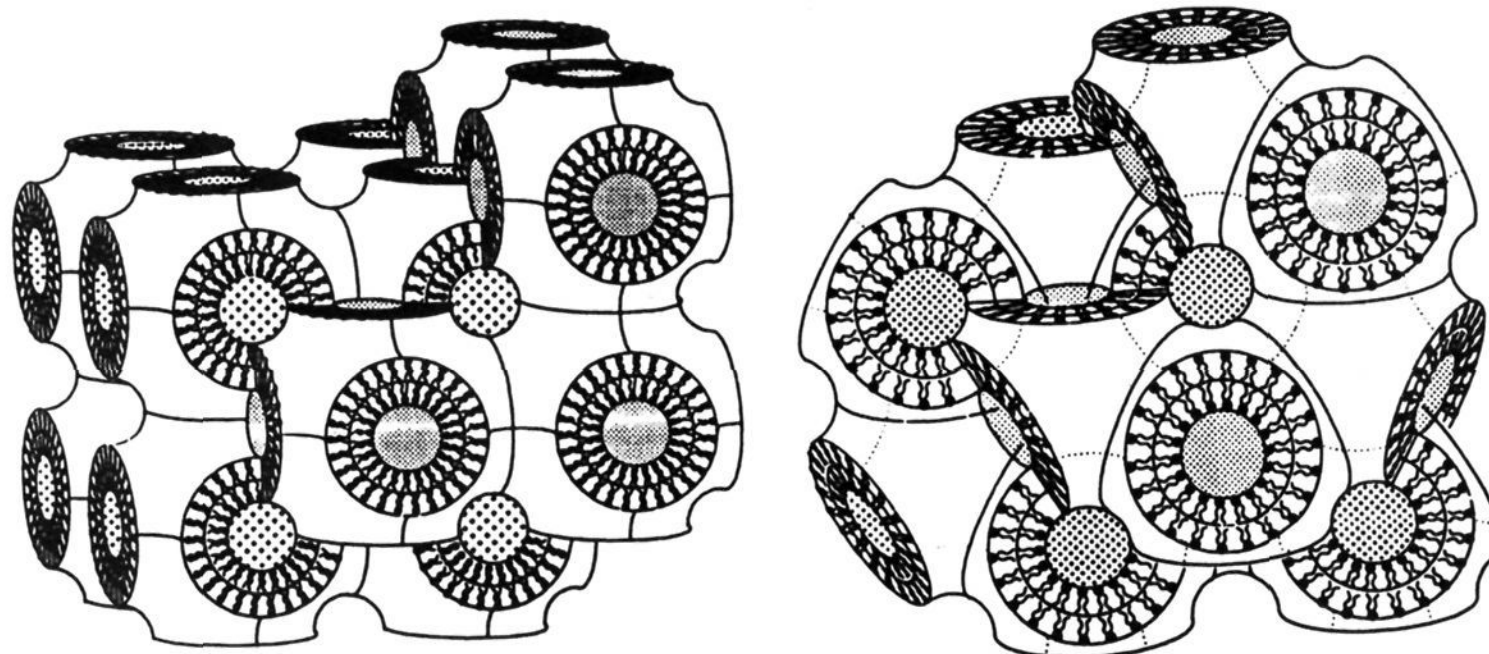


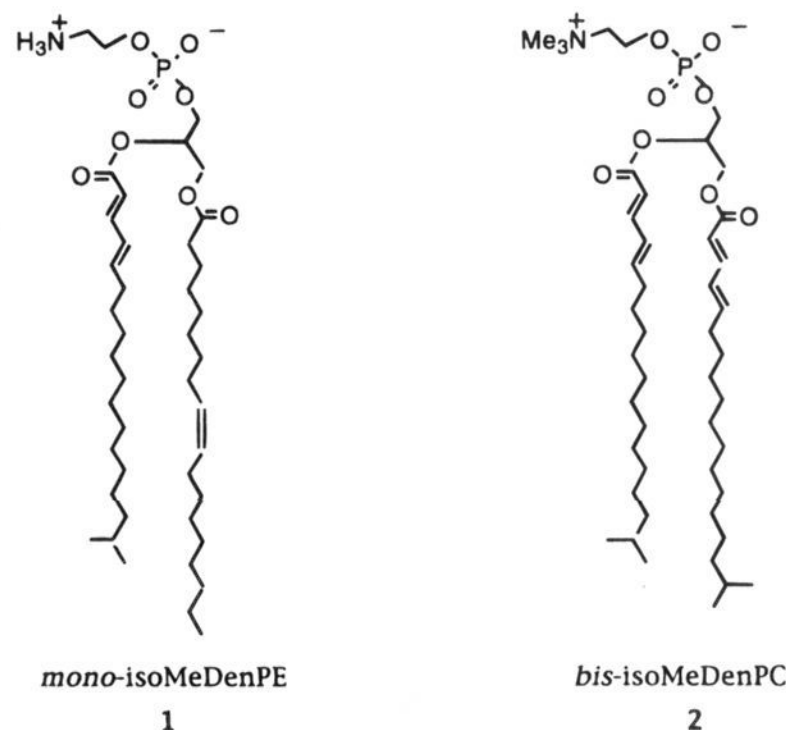
**Figure 1.** Schematic representations of bicontinuous cubic phases of lipids. Cross sections through the lipid surfaces are represented by concentric circles of the apposed amphiphiles. The two interpenetrating aqueous channels, shown by different dot patterns, are separated from each other by a continuous lipid bilayer surface. The connectivity of the aqueous regions is shown by the dot patterns. Left: Body centered cubic phase of the  $Im\bar{3}m$  space group. Right: Double diamond phase of the  $Pn\bar{3}m$  space group. (The graphics are provided courtesy of M. W. Tate et al., ref 3. Reprinted with permission from ref 3. Copyright 1991 Elsevier Science.)

reaction.<sup>12</sup> Several other reactive lipids, e.g. acryloyl, dienoyl, and sorbyl, may be polymerized by radical chain processes in either the  $L_\beta$  or  $L_\alpha$  phases. Lipids in the  $L_\alpha$  phase exhibit rapid lateral diffusion,<sup>13</sup> which appears to facilitate the polymerization process.<sup>14</sup> A series of systematic studies have provided new insights into the effect of the two-dimensional nature of the lipid bilayer on the rate and degree of polymerization in the  $L_\alpha$  phase.<sup>11,15–17</sup> Since the lateral diffusion coefficient for lipids in bicontinuous cubic phases is of the same order of magnitude as in the  $L_\alpha$  phase,<sup>18,19</sup> it was probable that similar polymerization strategies could be employed for both the  $L_\alpha$  and  $Q_{II}$  phases. Here we report the first successful stabilization of nonlamellar phases via the polymerization of the lipid region composed of reactive amphiphiles. An alternative approach which used monomers, e.g. styrene, dissolved within the wall of an amphiphilic assembly has previously been described.<sup>20</sup>

## Results and Discussion

Hydrated lipids which are known to form  $Q_{II}$  phases include certain phosphoethanolamine–phosphocholine (PE/PC) mixtures.<sup>1–3</sup> Therefore the polymerizable PE (**1**) and PC (**2**) shown in Chart 1 were designed and synthesized.<sup>21</sup> Reactive amphiphiles may have the polymerizable moiety located either in the hydrophilic head group, or near the lipid backbone, or in the hydrophobic lipid tail. We selected a reactive diene conjugated with the lipid acyl carbonyl, i.e. dienoyl group, in order to preserve the biocompatibility of the lipid–water interface and minimize the effect of the polymer chain on the

**Chart 1**



motions of the lipid tails. Radical-initiated polymerization of dienoyl lipids of this type has been reported to give degrees of polymerization of 25 to 50, whereas direct photopolymerization appears to produce oligomers.<sup>22</sup> The isomethyl branch at the chain terminus was incorporated into the structure in order to adjust the lamellar to nonlamellar phase transition temperature to a convenient range for the subsequent polymerization process. Previous studies by McElhaney and co-workers have demonstrated the effect of isomethyl substitution on lipid phase transitions.<sup>23,24</sup> Methyl substitutions at other locations along the acyl chain have even greater effects on the main phase transition temperature,  $T_m$ <sup>25,26</sup> and may prove useful in future studies.

(12) Lopez, E.; O'Brien, D. F.; Whiteside, T. H. *J. Am. Chem. Soc.* **1982**, *104*, 305–307.

(13) Fahey, P. F.; Webb, W. W. *Biochemistry* **1978**, *17*, 3046–3053.

(14) Kölchens, S.; Lamparski, H.; O'Brien, D. F. *Macromolecules* **1993**, *26*, 398–400.

(15) Sells, T. D.; O'Brien, D. F. *Macromolecules* **1994**, *27*, 226–233.

(16) Lei, J.; O'Brien, D. F. *Macromolecules* **1994**, *27*, 1381–1388.

(17) Lamparski, H.; O'Brien, D. F. *Macromolecules* **1995**, *28*, 1786–1794.

(18) Lindblom, G.; Larsson, K.; Johansson, L.; Fontell, K.; Forsén, S. *J. Am. Chem. Soc.* **1979**, *101*, 5465–5470.

(19) Eriksson, P.-O.; Lindblom, G. *Biophys. J.* **1993**, *64*, 129–136.

(20) Anderson, D. M.; Ström, P. In *Polymer Association Structures*; El-Nokaly, M. A., Ed.; ACS Symp. Ser. No. 384; American Chemical Society: Washington, DC, 1989; p 204.

(21) Lee, Y.-S.; Devanathan, S.; Srisiri, W.; O'Brien, D. F. *Chem. Phys. Lipids*, in revision.

(22) Tsuchida, E.; Hasegawa, E.; Kimura, N.; Hatashita, M.; Makino, C. *Macromolecules* **1992**, *25*, 207–212.

(23) Lewis, R. N. A. H.; Mannock, D. A.; McElhaney, R. N.; Turner, D. C.; Gruner, S. M. *Biochemistry* **1989**, *28*, 541–548.

(24) Lewis, R. N. A. H.; McElhaney, R. N. *Biochemistry* **1985**, *24*, 2431–2439.

(25) Lewis, R. N. A. H.; Sykes, B. D.; McElhaney, R. N. *Biochemistry* **1987**, *26*, 4036–4044.

(26) Menger, F. M.; Wood, M. G.; Zhou, Q. Z.; Hopkins, H. P.; Fumero, J. *J. Am. Chem. Soc.* **1988**, *110*, 6804–6810.

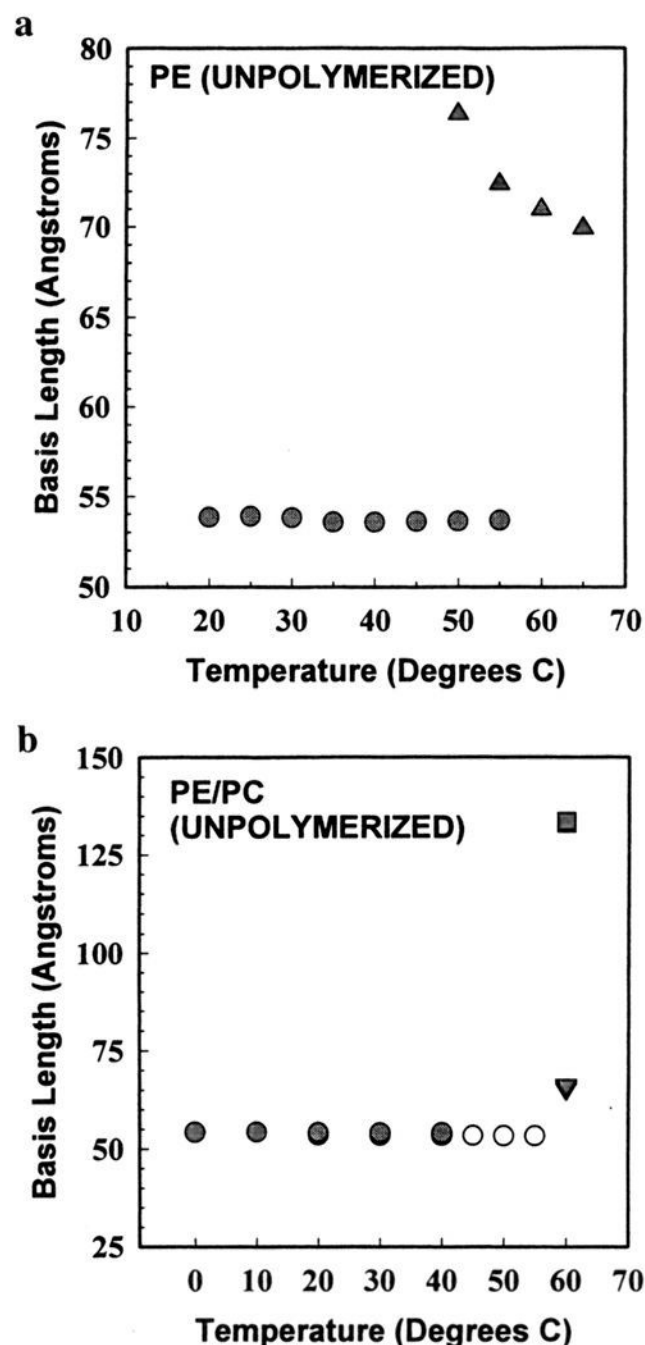


**Figure 2.** The basis lengths and lattices observed via X-ray diffraction are shown as a function of temperature. Circles indicate diffraction consistent with lamellar phases, triangles that with hexagonal phases, and squares that with cubic phases. (a) Unpolymerized PE upon heating. Note the presence of phase coexistence in the lamellar-hexagonal transition region. (b) Unpolymerized PE/PC = 3:1 upon heating. The open and closed symbols are for two different samples. The initially hexagonal signal slowly changes to cubic diffraction upon incubation at 60 °C.

The phase behavior of the individual hydrated PE or PC were examined. X-ray diffraction of the MilliQ water hydrated PE (1) (ca. 300 mg/mL) revealed the existence of an  $L_{\alpha}$  phase from 20 to 55 °C with a  $d$ -spacing (e.g., lattice basis vector length) of 5.37 nm and the onset of an  $H_{II}$  phase at ca. 55 °C. The  $d$ -spacing was 7.10 and 6.99 nm at 60 and 65 °C, respectively (Figure 2a). Differential scanning calorimetry of the PE (10 mg/mL) over the temperature range 20 to 75 °C showed a thermotropic endotherm at 56.5 °C. The coincidence of the X-ray and DSC data indicate this endotherm marks the transition from the  $L_{\alpha}$  to the  $H_{II}$  phase for the PE. The hydrated PE sample changed in appearance from a uniform turbid suspension at room temperature to a thin buoyant film on excess water at temperatures greater than 55 °C. A thermotropic endotherm was observed at 7.2 °C for the hydrated PC (2). No other transitions were detected below 70 °C. This transition temperature is reasonable for the  $T_m$  based on comparisons to other substituted PCs.<sup>23,24</sup> The hydrated PC was a white suspension typical of bilayer membranes.

A 3:1 molar mixture of the PE/PC was hydrated in a glass ampule with MilliQ water at either low (25 to 100 mg/mL) or high concentration (180 to 500 mg/mL). Hydration of the

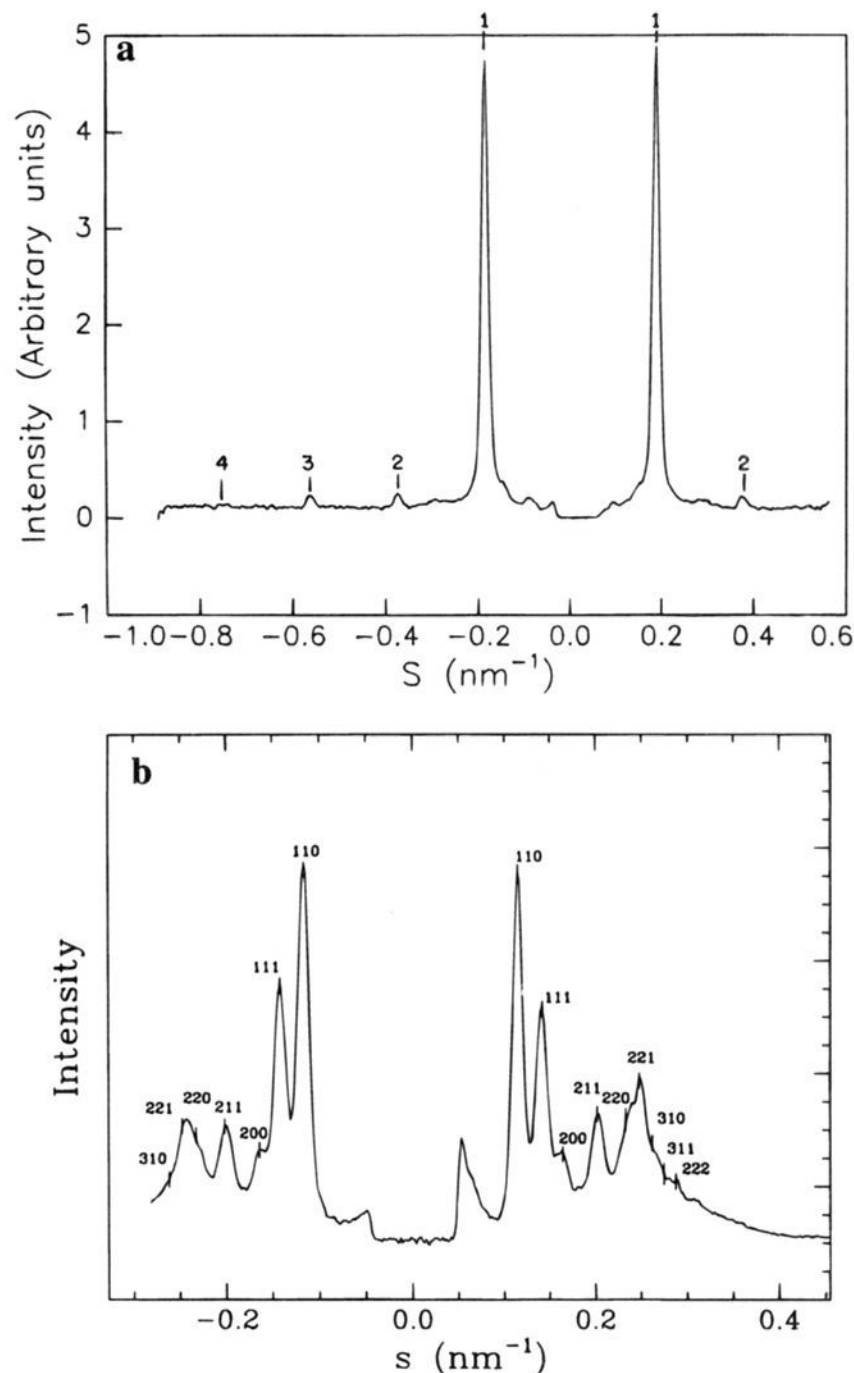


**Figure 3.** Densitometrization of the two-dimensional X-ray diffraction pattern of a hydrated 3:1 molar mixture of 1 and 2 (500 mg/mL) at (a) 20 °C and (b) after incubation at 60 °C for 12 h. The tic marks indicate the expected positions from a lamellar lattice (a) of basis length 5.36 nm and from a  $Pn\bar{3}m$  lattice (b) of basis length 12.2 nm.

samples was accomplished by heating at 45 °C, vortexing, then cooling to -77 °C several times. A white homogenous suspension of bilayers was formed upon hydration. The high-concentration samples were characterized by X-ray diffraction (Figure 2b). The sample at 20 °C showed prominent peaks consistent with diffraction patterns obtained from a lamellar lattice (Figure 3a). The sample maintained its lamellar character at temperatures up to 55 °C. Upon incubation at 60 °C the diffraction pattern progressively changed over 12 h from a hexagonal phase pattern to the stable pattern shown in Figure 3b. The new pattern is inconsistent with either a lamellar or an inverted hexagonal phase. Rather the peak positions with a  $d$ -spacing of 12.2 nm are consistent with a bicontinuous cubic phase of  $Pn\bar{3}m$  symmetry, similar to that observed in other hydrated PE/PC systems.<sup>3,27</sup> If the temperature of the sample was lowered below 55 °C, the sample reverted to lamellar phase diffraction, albeit with some hysteresis.

The low-concentration PE/PC samples were characterized by <sup>31</sup>P NMR spectroscopy before polymerization. The NMR of the unpolymerized sample (100 mg of lipid/mL) at 25 °C exhibited a line shape characteristic of the  $L_{\alpha}$  phase. The baseline width (44 ppm) of the pattern corresponded to that of

(27) Barry, J. A.; Lamparski, H.; Shyamsunder, E.; Osterberg, F.; Cerne, J.; Brown, M. F.; O'Brien, D. F. *Biochemistry* **1992**, *31*, 10114-10120.

DOPC which is known to exist in the  $L_{\alpha}$  phase at this temperature. A small isotropic signal was also present in the spectrum that may possibly be due to some small vesicles in the NMR sample. The sample was heated rapidly and then incubated at the new temperature prior to acquisition of each spectrum which remained unchanged over a period of at least 3 h at 35, 45, and 53 °C. At 55 °C the isotropic signal increased slightly. At 57 °C the spectrum became predominately isotropic with some residual  $L_{\alpha}$  component. An additional feature was the appearance of a peak downfield of the isotropic signal with a similar intensity to that of the  $L_{\alpha}$  portion. This signal was probably due to the presence of some lipid in the  $H_{II}$  phase. At 60 °C the signal due to the lamellar phase disappeared and the proportion ascribed to the  $H_{II}$  phase diminished compared to the isotropic signal. The isotropic signal was preferentially enhanced by incubation for 12–15 h at 60 or 65 °C. The full-width at half-maximum (fwhm) of the isotropic signal was ca. 2 ppm. After the unpolymerized sample was cooled to 25 °C within the NMR probe for 12 h, a new spectrum showed a predominately  $L_{\alpha}$  line shape with a baseline width of 44 ppm. An isotropic signal was also present in a larger proportion than the original preheated sample. The white sample was homogeneous and opaque after removal from the instrument, indicating the reversion from nonlamellar to lamellar lipid structures. The NMR studies indicate that incubation of the 3:1 PE/PC sample at 60 °C forms a nonlamellar lipid phase, which is presumably the same bicontinuous cubic phase observed in the X-ray study. Furthermore, these data show the nonlamellar phase is unstable after cooling and incubation at room temperature.

Polymerization studies of the nonlamellar phase were performed at low lipid concentration (25 mg/mL). The sample was brought to room temperature, flushed with argon, sealed with a rubber septum, then incubated in a shaking water bath at 60 °C for 15 h. The sample appearance changed during the incubation from an opaque suspension of bilayers to a compact white structure surrounded by an excess of clear aqueous medium suggestive of an inverted nonlamellar phase, i.e. hydrocarbon continuous in excess water. If the sample was cooled to room temperature prior to polymerization, then the bilayer appearance returned. Polymerization of the sample in the nonlamellar phase was affected by the addition of potassium persulfate and sodium bisulfite to the excess water and continued incubation at 60 °C for 6 h. Decomposition of the persulfate in the water yields hydroxyl radicals which are free to diffuse into the nonlamellar phase to react with the lipid dienoyl groups. The redox polymerization of similar dienoyl lipids in the  $L_{\alpha}$  phase produced polymers with a degree of polymerization of ca. 30.<sup>22</sup> The sample solubility in organic solvents was tested before and after polymerization. The unpolymerized lipid mixture was soluble in several organic solvents at room temperature including chloroform, dichloromethane, 1,1,1,3,3,3-hexafluoro-2-propanol (HFIP), and tetrahydrofuran (THF). The conversion to polymer after polymerization was determined by chloroform extraction of a known weight of the freeze-dried lipid, followed by determination of the intensity of the dienoyl absorption at 263 nm. The solubility of the sample was generally complete in each of the above solvents when the conversion to polymer was 60% or less. When the conversions to polymer were greater than 80% the polymeric material was insoluble in all organic solvents, including HFIP, in a manner consistent with cross-linking of the lipids. Furthermore the highly polymerized samples remained in a nonlamellar structure after dilution and agitation or after storage near 0 °C for days, well below the lamellar to nonlamellar transition temperature.

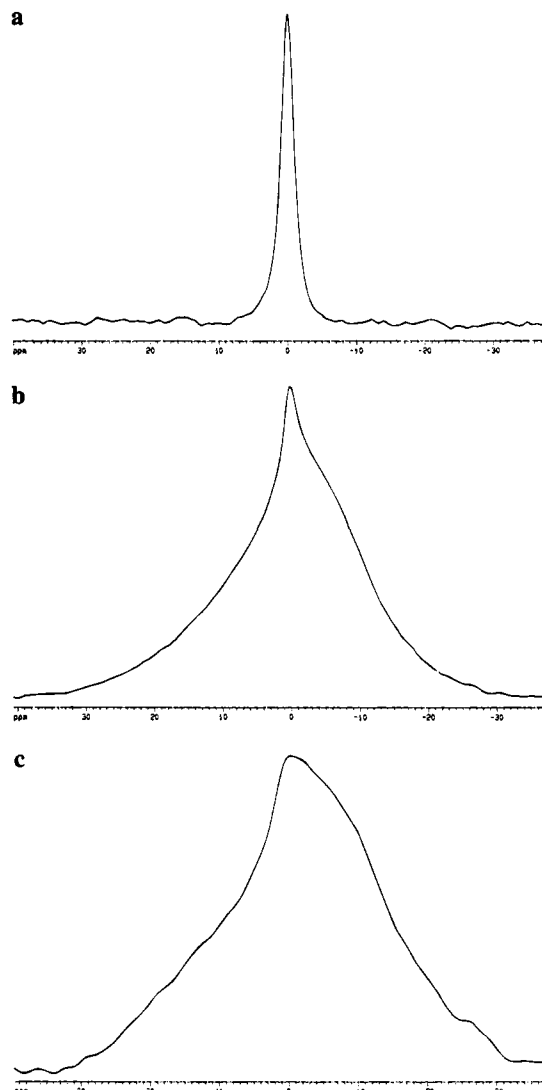


**Figure 4.**  $^{31}\text{P}$  NMR spectra of a hydrated 3:1 molar mixture of **1** and **2**: (a) unpolymerized sample after incubation at 65 °C; (b) polymerized (96% conversion) sample at 65 °C; (c) polymerized sample at 27 °C.

These data indicate that stabilization of the nonlamellar phase of the 3:1 PE/PC samples requires high conversion to polymer. At low conversions the polymers created in the nonlamellar phase are likely to be linear and organic soluble. This appears to be a consequence of the relatively inefficient cross-linking of bis-substituted lipids. Previous studies by Kölcens et al. found that a mole fraction of ca. 0.3 bis-substituted lipid was necessary to cross-link a mixture of mono- and bis-substituted acryloyl lipids.<sup>14</sup> Although the cross-linking efficiency of dienoyl lipids remains to be determined, it is likely that a similar proportion of bis-dienoyl lipid is necessary for sample gelation due to cross-linking. Thus, under the polymerization protocols used in this study, only the high conversion to polymer conditions were effective in stabilizing the nonlamellar lipid structure.

The polymer sample (25 mg/mL) was also characterized by  $^{31}\text{P}$  NMR spectroscopy. Prior to polymerization at 65 °C an isotropic signal was observed with a 4 ppm fwhm (Figure 4a). The initiator chemistry was added to the NMR sample and incubated for 4 h during which time spectra were acquired. Polymerization of the incubated NMR sample resulted in a progressive broadening of the original isotropic signal, which is an expected consequence of the decreased lateral diffusion of the polymerized lipids. The spectrum of the 4 h polymerized sample at 65 °C consisted of a broad somewhat symmetrical



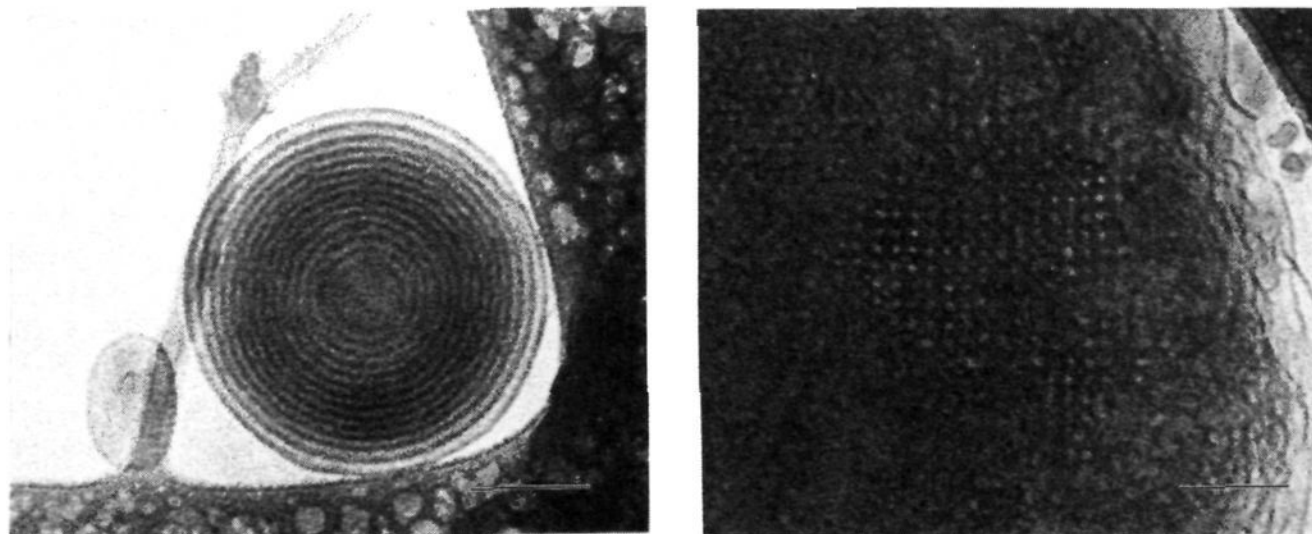


**Figure 5.** Cryo-transmission electron micrographs of a hydrated 3:1 molar mixture of lipids **1** and **2** (25 mg/mL) before (a, left) and after (b, right) conversion from lamellar to nonlamellar structures. Sample b was polymerized. The dark border images are due to the lattice of the lacy carbon grid. Scale bars: (a) 100 nm; (b) 100 nm.

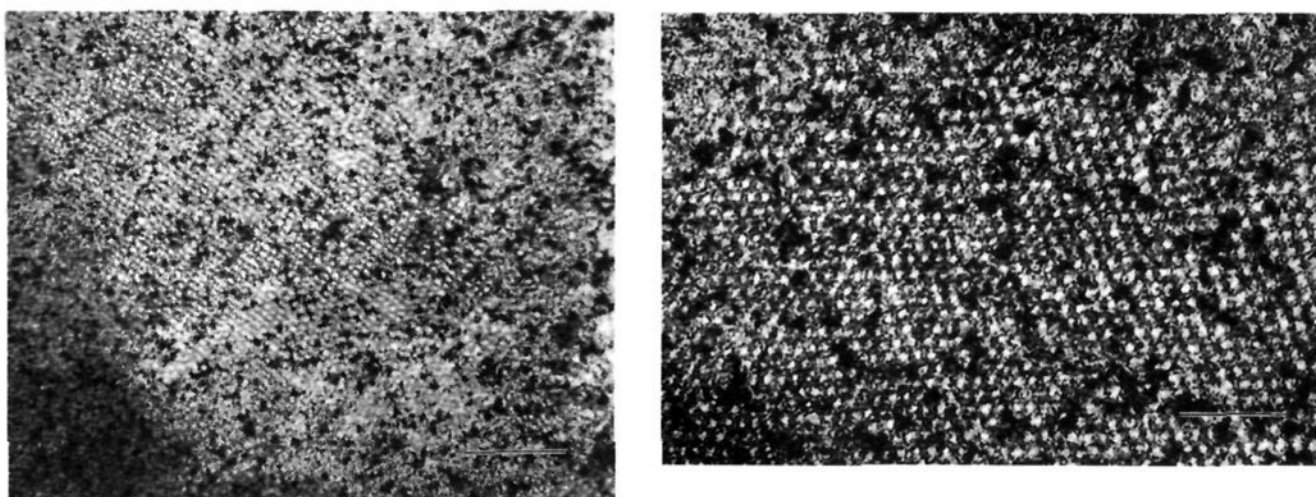


**Figure 6.** Transmission electron micrographs of stained thin sections after polymerization of a 60 °C incubated sample of a 3:1 molar mixture of lipids **1** and **2**. The unstained light areas are assigned to the aqueous channels. The black areas are due to excess stain. Scale bars: (a, left) 200 nm; (b, right) 100 nm.

line shape with a 15 ppm fwhm (Figure 4b). The sample was subsequently allowed to cool to 27 °C and incubated for 3 h (Figure 4c). The spectrum of the polymerized sample at 27 °C was similar but broader than that at 65 °C.

Cryo-TEM shows multilamellar liposomes prior to conversion to nonlamellar structures (Figure 5a). After sample incubation at 60 °C and polymerization the cryo-TEM revealed an entirely different structure. The relatively small structure shown in Figure 5b was selected from the periphery of a larger nonlamellar structure because its dimensions permitted observation of the structure. Although this sample varies in thickness, several regions of a square lattice can be seen indicating the presence of multidomains of lipid in a state suggestive of a cubic phase. Another larger sample of the polymerized material was stained with osmium tetroxide, embedded, and microtomed to yield thin 90 nm sections. Transmission electron microscopy of these thin sections generally showed square or hexagonal lattices throughout all the fields of view. The hexagonal lattices were too large to be consistent with the X-ray determined  $H_{II}$  phase and were more consistent with a section across a cubic phase. Several images were recorded photographically and representative examples of two areas that have different spacings are shown in Figure 6. In each TEM the unstained regions are ascribed to aqueous regions or channels. The apparent diameter of the channels in the micrographs is  $6 \pm 1$  nm. The center-to-center distance between channels ranges from 17 to 18 nm in Figure 6a, whereas it is 12–13 nm in Figure 6b. These data indicate the polymerized lipid assembly consists of a polydomain nonlamellar structure. The variation in TEM repeat distances could be due to different cutting planes through the polymerized sample, changes induced upon specimen preparation for TEM, and/or the existence of nonlamellar structures corresponding to

different spaces groups. Unfortunately the polydomain nature of these samples, in conjunction with weak diffraction, has precluded an unambiguous X-ray characterization. It is not unusual for lamellar lipid structures to collapse into a concentrated polydomain nonlamellar phase in the presence of excess water. We cannot exclude the possibility of multidomain formation due at least in part to the multiple initiation sites of the polymerization process. Efforts to form and polymerize monodomain nonlamellar phases are in progress.

One such study was performed at high concentration with a 3:1 PE/PC sample in an X-ray capillary, which was taken to 60 °C, where an inverted hexagonal phase was formed initially (see Figure 2b). After sample polymerization it exhibited a stable  $H_{II}$  pattern and displayed no lamellar phase diffraction over the temperature range 20–60 °C. The striking characteristic of this polymerized  $H_{II}$  phase is the lack of change in the dimensions of the phase with temperature (Figure 7). This contrasts with typical  $H_{II}$  phases which change dimensions dramatically with temperature.<sup>3</sup>

In summary we have described the first representatives of a new family of materials with interpenetrating water channels with high surface area and potentially bicompatible lipid–water interfaces. These results indicate the general strategy can be successfully employed to stabilize nonlamellar lipid assemblies. We are currently evaluating this approach with additional polymerizable amphiphiles to create novel stabilized  $Q_{II}$  as well as  $H_{II}$  phases. This method is distinct yet complementary to the recently reported templating method for the formation of mesoporous molecular sieves.<sup>28</sup> The ability to form stable bicompatible materials with aqueous pore sizes which are in order of magnitude larger than those observed with inorganic zeolites should provide opportunities for incorporating relatively

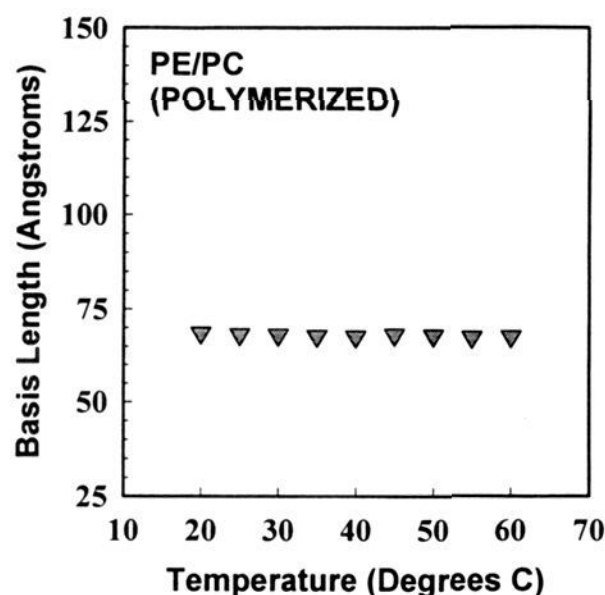


**Figure 7.** The basis length and lattices as a function of temperature for a PE/PC = 3:1 sample polymerized in the hexagonal phase at 60 °C. The basis lengths were measured as the sample was cooled from the polymerization temperature.

large synthetic or biological molecules into the channels in a manner that has already proven especially useful in microporous solids.

## Experimental Section

**Methods and Materials.** Compounds containing a UV-sensitive group were handled under yellow light. UV-visible absorption spectra were recorded on a Varian DMS 200 spectrophotometer. A Microcal Inc. Model MC-2 differential scanning calorimeter was used to determine the lipid phase transition temperatures.

**(a) Lipids.** The polymerizable isomethyl branched dienoic acid was synthesized by coupling isobutyl Grignard with THP protected 11-bromo-1-undecanol, followed by deprotection, oxidation to the aldehyde, reaction with triethyl 4-phosphonocrotonate, and controlled hydrolysis. The column purified acid was used to acylate t-Boc protected 1-oleoyl-2-hydroxy-*sn*-glycero-3-PE, which was subsequently deprotected to give the mono-isoMeDenPE **1**. L- $\alpha$ -GlyceroPC was acylated with the same dienoic acid to yield the bis-isoMeDenPC **2**. The synthetic procedures will be reported elsewhere.<sup>21</sup>

**Phase Behavior of Unpolymerized Lipids.** **(a) <sup>31</sup>P NMR.** A 3:1 PE/PC lipid sample was fully hydrated in 0.5 mL of Milli-Q water to a concentration of 100 mg/mL. The hydrated lipid was sealed in an 8-mm tube which was placed into a 10-mm NMR tube. The sample temperature was controlled to  $\pm 0.2$  °C with the variable temperature of the NMR instrument. The sample was incubated at the acquisition temperature for 15 min for every 2.5 °C increase in the temperature. Proton-decoupled <sup>31</sup>P NMR spectra were acquired on a General Electric GN-300 spectrometer operating at 121.7 MHz (7.0 T) using the procedure described in Barry et al.<sup>27</sup> A phase-cycled pulse sequence ( $90^\circ - \tau_1 - 180^\circ - \tau_2 - \text{acquisition}$ ) was used with a  $90^\circ$  pulse length of 11  $\mu\text{s}$ , the delay  $\tau_1$  of 100  $\mu\text{s}$ , the time before acquisition  $\tau_2$  of 40  $\mu\text{s}$ , and the delay between sequences of 1 s. The free induction decays consisted of 2000–8000 scans and were multiplied by a line broadening of 80 Hz before Fourier transformation.

**(b) X-ray Diffraction.** Lipid samples of PE/PC (3:1) were fully hydrated to concentrations of 180 to 500 mg/mL. The hydrated samples were loaded in a dark room into X-ray capillary tubes and sealed. X-ray diffraction data were obtained using a Rigaku RU-200 rotating anode X-ray machine equipped with a microfocus cup. The generated Cu K $\alpha$  X-rays were focussed via bent mirror optics. Two-dimensional X-ray images were collected with the Princeton SIT area detector as described previously.<sup>29,30</sup> The digital powder diffraction images were

azimuthally integrated along an arc  $\pm 10^\circ$  from the meridional axis to generate plots (e.g., Figure 3) of scattered intensity versus  $S = 2 \sin\theta / 1.54 \text{ \AA}$  where  $2\theta$  is the angle between the incident and scattered beam directions.

**Polymerized Lipid Samples.** **(a) Polymerization.** Potassium persulfate (300 mg, 1.1 mmol) and sodium bisulfite (115 mg, 1.1 mmol) were diluted to 10 mL with MilliQ water. A volume of this solution was added to the thermally incubated lipid sample to give  $[M]/[I] = 10$ , where  $[M]$  represents the concentration of dienoyl groups. The lipid sample in excess water with added initiator was incubated at 60 or 65 °C for up to 6 h. The conversion to polymer as a function of time was determined by polymerization of known lipid weight aliquots, followed by sample freeze-drying and then chloroform extraction of the solid sample. The UV-absorption intensity due to the dienoyl chromophore was measured spectrophotometrically.

**(b) <sup>31</sup>P NMR.** A hydrated PE/PC (3:1) lipid sample (0.5 mL at 25 mg/mL) was incubated at 60 °C for 15 h with gentle agitation. The sample was sealed in an 8-mm tube which was placed into a 10-mm NMR tube to determine the spectrum of the unpolymerized sample. Polymerization was started by the addition of a 84- $\mu\text{L}$  aliquot of initiator solution to the NMR sample. Additional spectra were acquired at the times and temperatures indicated in the Results. The proton-decoupled <sup>31</sup>P NMR spectra were acquired on a Bruker 400 spectrometer operating at 161.97 MHz (9.4 T). The temperature was controlled to  $\pm 0.2$  °C. A phase-cycled pulse sequence ( $90^\circ - \tau_1 - 180^\circ - \tau_2 - \text{acquisition}$ ) was used as above. The free induction decays consisted of 1200–40000 scans and were multiplied by a line broadening of 200 or 500 Hz before Fourier transformation.

**(c) Electron Microscopy.** Samples for cryo-TEM were prepared by application of a 4- $\mu\text{L}$  sample (25 mg/mL) to a 300-mesh copper grid with a lacy substrate at the appropriate temperature. The excess liquid was blotted by gently moving the grid horizontally across a pre-moistened Whatman No. 1 filter paper. The filter paper was pre-moistened in the same solution that the assemblies were suspended. The blotting process was monitored under a dissection microscope until bulk fluid was no longer visible on either side of the grid. A thin film of sample then spanned the surface of the lacy substrate. Immediately after formation of this thin film, the sample was plunge-frozen in liquid propane. The samples were analyzed using a Gatan Model 626 cryotransfer system and a Phillips EM 420 electron microscope at 120 kV and a sample temperature of  $-165$  to  $-170$  °C. The quality of the vitrified sample, i.e. the absence of hexagonal and/or cubic ice crystals in the preparation, was checked by electron diffraction. Care was taken that the frozen sample was exposed to a minimum dose of electrons before photography. Images were recorded photographically at an instrument magnification between 18500X and 36000X and at 0, 1.2, and 2.4  $\mu\text{m}$  underfocus.

Polymerized lipid samples for ultramicrotomy were fixed for 2 h in 1% osmium tetroxide in distilled water at room temperature, washed, sequentially dehydrated with ethanol, and exchanged into LR White. The sample was embedded by placing the material in gelatin capsules in fresh LR White resin and then letting capsules sit for 8 h at room temperature and then cure for 2 days at 60 °C. The sections were cut 90 nm thick on a diamond knife on a Reichert Ultracut-E and placed on 150-mesh uncoated copper grids. The sections were subsequently stained with 5% uranyl acetate in 50% methanol in water for 10 min and Reynolds lead citrate for 3 min. The sections were observed on a Phillips EM 420 electron microscope at 75 kV.

**Acknowledgment.** The authors thank the NSF-CTS (D.F.O.), DOE, and NIH (S.M.G.) for support of this research. We thank Constantin Job and Michael F. Brown for assistance with <sup>31</sup>P NMR spectra and John C. Gilkey, David L. Bentley, and Beth Huey for their assistance with electron microscopy and the micrographs.

JA9502738

(28) Beck, J. S.; Vartuli, J. C.; Roth, W. J.; Leonowicz, M. E.; Kresge, C. T.; Schmitt, K. D.; Chu, C. T.-W.; Olson, D. H.; Sheppard, E. W.; McCullen, S. B.; Higgins, J. B.; Schlenker, J. L. *J. Am. Chem. Soc.* **1992**, *114*, 10834–10843.

(29) Gruner, S. M.; Milch, J. R.; Reynolds, G. T. *Rev. Sci. Instrum.* **1982**, *53*, 1770–1778.

(30) Gruner, S. M.; Milch, J. R.; Reynolds, G. T. *Nucl. Instrum. Methods Phys. Res.* **1982**, *195*, 287–297.